

This article was downloaded by: [Neeti Kapur]

On: 04 July 2011, At: 08:50

Publisher: Taylor & Francis

Informa Ltd Registered in England and Wales Registered Number: 1072954 Registered office: Mortimer House, 37-41 Mortimer Street, London W1T 3JH, UK



Molecular Simulation

Publication details, including instructions for authors and subscription information:

<http://www.tandfonline.com/loi/gmos20>

First-principles study of CO oxidation on bismuth-promoted Pt(111) surfaces

Neeti Kapur ^a, Bin Shan ^a, Jangsuk Hyun ^a, Ligen Wang ^a, Sang Yang ^a, John B. Nicholas ^a & Kyeongjae Cho ^b

^a Nanostellar Inc., 3696 Haven Avenue, Redwood City, CA, 94063, USA

^b Department of Material Science and Engineering and Department of Physics, University of Texas at Dallas, Richardson, TX, 75080, USA

Available online: 04 Jul 2011

To cite this article: Neeti Kapur, Bin Shan, Jangsuk Hyun, Ligen Wang, Sang Yang, John B. Nicholas & Kyeongjae Cho (2011): First-principles study of CO oxidation on bismuth-promoted Pt(111) surfaces, *Molecular Simulation*, 37:8, 648-658

To link to this article: <http://dx.doi.org/10.1080/08927022.2010.543978>

PLEASE SCROLL DOWN FOR ARTICLE

Full terms and conditions of use: <http://www.tandfonline.com/page/terms-and-conditions>

This article may be used for research, teaching and private study purposes. Any substantial or systematic reproduction, re-distribution, re-selling, loan, sub-licensing, systematic supply or distribution in any form to anyone is expressly forbidden.

The publisher does not give any warranty express or implied or make any representation that the contents will be complete or accurate or up to date. The accuracy of any instructions, formulae and drug doses should be independently verified with primary sources. The publisher shall not be liable for any loss, actions, claims, proceedings, demand or costs or damages whatsoever or howsoever caused arising directly or indirectly in connection with or arising out of the use of this material.

First-principles study of CO oxidation on bismuth-promoted Pt(111) surfaces

Neeti Kapur^{a*}, Bin Shan^a, Jangsuk Hyun^a, Ligen Wang^a, Sang Yang^a, John B. Nicholas^a and Kyeongjae Cho^{b*}

^aNanostellar Inc., 3696 Haven Avenue, Redwood City, CA 94063, USA; ^bDepartment of Material Science and Engineering and Department of Physics, University of Texas at Dallas, Richardson, TX 75080, USA

(Received 26 September 2010; final version received 25 November 2010)

Vehicle emission control regulations necessitate the removal of carbon monoxide (CO) from engine exhausts via CO oxidation. Although bismuth (Bi)-promoted platinum (Pt) catalysts show improvement in CO oxidation performance over pure Pt, it is still not known whether Bi acts simply as a site blocker to reduce CO poisoning or whether it is an active participant in the catalytic reactions. In this study, we report density functional theory-based CO oxidation energetics and kinetics in the presence of different Bi dopant configurations. Adsorption energies for both CO and oxygen atoms are found to be reduced by Bi doping. Bi dopant also creates surface areas in its vicinity where CO adsorption is prohibited, whereas molecular oxygen dissociation is promoted. Significant reduction is shown for CO oxidation barriers on Bi-modified Pt(111) surfaces leading to exothermic CO₂ formation. Our results elucidate that promoting Pt with Bi affects both the electronic properties of the catalyst and alters the Pt ensemble size available for elementary reactions within CO oxidation mechanism.

Keywords: DFT; bismuth; CO; oxidation; catalysis

1. Introduction

Platinum (Pt) is one of the most active transition metal catalysts widely used for converting carbon monoxide (CO) pollutant within diesel engine exhaust stream to carbon dioxide (CO₂). It is commonly accepted that CO oxidation proceeds via Langmuir–Hinshelwood (LH) mechanism on Pt surface, which involves CO adsorption and desorption, molecular oxygen (O₂) dissociation and surface reaction between CO and atomic oxygen (O). Adsorbed CO molecules equilibrate to a saturation coverage of 0.5 monolayer (ML) on Pt(111) under cold start conditions, which was confirmed both theoretically [1] and experimentally with scanning tunnelling microscopy and electron energy loss spectroscopy [2–4]. CO desorption is hence considered to be the rate-limiting step and a prerequisite for O₂ adsorption and dissociation. Apparent O₂ dissociation barrier is also reported to increase with local CO coverage due to the intermolecular CO–O₂ repulsions [5–7]. Thus, intrinsic CO oxidation activity on Pt can be improved with dopants which promote CO desorption and reduce O₂ dissociation barrier.

Platinum–bismuth (Bi) catalysts are known to improve selectivity for partial oxidation of cinnamylalcohols to cinnamaldehydes [8], promote oxidative dehydrogenation of alcohols and polyols to carbonyls and carboxylic acids [9] and enhance oxidation of hydroxyl group in glycerols [10]. Although Bi dopant is inactive by itself for oxidation reactions, it is proposed to have a geometric blocking effect which decreases Pt ensemble size for undesired reactant adsorption. Bi addition is

reported to suppress CO poisoning on Pt surface [11] leading to significant improvement in direct alcohol fuel cell efficiency [12] even for low Bi coverage [13]. CO electrooxidation kinetics for irreversibly bound Bi atoms on Pt electrodes are of negative order for CO partial pressure [14], indicating that surface poisoning effect has been suppressed but not eliminated. Furthermore, experimental studies have verified that Bi-promoted Pt catalyst is effective for CO oxidation under diesel exhaust conditions [15,16]. The light-off temperature (temperature at which conversion of 50% CO to CO₂ is achieved) is reduced considerably (60–70°C) on Bi-promoted Pt surface as compared with that on pure Pt (237°C) and this improvement depends on the Bi/Pt loading ratio [16]. Although previous reports have suggested that Bi simply blocks CO binding sites, there is no clear evidence to rule out simultaneous electronic effect on reaction energetics and kinetics. To elucidate these possibilities, we focus on resolving electronic and geometric effects of alloying Pt surface with Bi dopant and their impact on CO oxidation mechanism within this study.

Qualitatively, Pt–Bi/alumina catalysts can include both reduced and oxidised Bi species. Although Bi exists as Bi³⁺ under ambient conditions as revealed by X-ray absorption spectroscopy, it can be reversibly reduced to Bi⁰ if the dopant resides on Pt surface [9]. Therefore, Bi dopant is likely to exist in both reduced and partially oxidised form depending on catalyst preparation methods and reaction conditions.

*Corresponding authors. Email: nkapur@nanostellar.com; kjcho@utdallas.edu

Bismuth metal readily oxidises at low temperatures to Bi_2O_3 , which has a complex crystallographic structure [12]. Electron diffraction and X-ray photoelectron spectroscopic (XPS) studies [17] have also confirmed bismuth suboxide (BiO) formation within thin bismuth oxide films. However, it is not clear whether oxygen atoms bonded to Bi are chemically reactive. Propene and butane oxidation on bismuth oxide compounds [18,19] proceeds only in the presence of molecular oxygen because strong Bi–O bonds prevent oxygen removal from the cluster. On the other hand, catalyst potential measurements on Pt–Bi bimetallic catalysts demonstrate that the catalyst is in partially oxidised state but is not inactive towards partial oxidation of alcohols [8]. Despite the indication that Bi dopant can exist in oxide form, there has been no explicit examination of these suboxides and their effect on reaction mechanism.

In this work, we investigate the role of bismuth dopant in promoting CO oxidation on Pt surfaces using density functional theory (DFT). We examine Bi configurations both as a surface dopant and as an adatom on Pt(111) surface to deduce electronic and geometric effects on adsorbate energetics. Comparisons are drawn between Pt(111) and Bi doped Pt(111) to elucidate reaction kinetics and validate preferential catalytic mechanisms.

2. Computational methodology

Ground-state energies for the adsorbed systems were determined by using self-consistent, gradient-corrected DFT as implemented in Vienna *ab initio* simulation package [20]. A three-layered slab was used to model $p(2 \times 2)$, $p(4 \times 4)$ and orthogonal (4×4) unit cells of Pt(111) surface with the metal atoms in the bottom layer fixed at the bulk positions. Bi promoter atoms were modelled as adatoms on Pt(111) surface and also as a surface dopant replacing a Pt atom in the top layer of the metal slab. These calculations were run in cubic supercells with at least 10 \AA of vacuum between atoms in neighbouring cells to ensure negligible periodic image interaction. A $4 \times 4 \times 1$ Monkhorst–Pack mesh was used for sampling the Brillouin zone for $p(2 \times 2)$ unit cell, whereas $2 \times 2 \times 1$ mesh was used for $p(4 \times 4)$ and orthogonal (4×4) unit cell surfaces [21]. Plane waves with 400 eV as cut-off energy were used to describe the electronic wave functions, and projector augmented wave (PAW) pseudopotentials [22] were used to describe electron–ion interactions. Revised Perdew–Burke–Ernzerhof (RPBE) functional form of generalised gradient approximation was used for calculating the exchange–correlation energies. Binding energies (BEs) were calculated using the following equation:

$$\text{BE} = E_{\text{total}} - E_{\text{substrate}} - E_{\text{molecule}}, \quad (1)$$

where E_{total} refers to the energy of total system, $E_{\text{substrate}}$

refers to the metal slab energy and E_{molecule} refers to species in vacuum. Dimer method [23] was used to find the transition state (TS) structures for reactions examined in this study, and the initial direction along the dimer was generated, based on the reaction products. Imaginary frequencies were used to confirm these configurations and the apparent activation barriers (E_a) were determined from the equation:

$$E_a = E_{\text{TS}} - E_{\text{IS}}, \quad (2)$$

where E_{TS} corresponds to TS energy and E_{IS} refers to reactant energy. Bader charge analysis [24] was performed to examine charge redistribution and net charge transfer due to Bi doping on Pt(111) surface. Net electron transfer was determined from Equation (3)

$$\Delta n = n_{\text{total}} - n_{\text{Pt surface}} - n_{\text{Bi}}, \quad (3)$$

where Δn corresponds to net charge transfer, n_{total} corresponds to Bader charge for doped Pt surface, n_{surface} corresponds to Bader charge for Pt(111) surface and n_{Bi} corresponds to Bader charge for Bi atom.

3. Results and discussion

We have first examined the stable dopant configurations for Bi, both as surface alloy and as an adatom on Pt(111). Subsequently, we have determined the adsorption energies for reactants (CO and O_2 molecules) and products (O) and ascertained TS structures for CO oxidation routes on doped Pt(111) surfaces.

3.1 Bi dopant configurations on Pt(111) surface

Figure 1(a) and (c) shows the top and side views for $\text{Pt}_3\text{Bi}/\text{Pt}(111)$ surface alloy structure examined in this study such that Bi replaces a Pt atom in the top layer of the metal slab ((2×2) unit cell). Since Bi atom has a larger atomic radii (3.09 \AA) than Pt(111) lattice (2.78 \AA), this dopant introduces strain in the Pt substrate and protrudes *ca.* 0.7 \AA above the surface plane. The bond distances between Pt atoms within the top layer of this PtBi surface alloy are determined to be 2.790 \AA and 2.851 \AA , as compared to Pt–Pt distance of 2.820 \AA within the Pt(111) surface.

Four stable binding sites (atop, bridge, fcc and hcp) were considered for Bi adatom adsorption on Pt(111) surface. Bi adsorption on both fcc and hcp sites on Pt(111) corresponds to the lowest energy configuration with a BE of -383 kJ/mol (0.25 ML Bi coverage). Figure 1(b) and (d) shows the representative Bi adatom/Pt(111) structure with dopant atoms bound on hcp sites. All three Pt–Bi bond lengths are equivalent to 2.678 \AA in this configuration. Bi binding on Pt(111) surface was found to further

strengthen to -396 kJ/mol with a decrease in Bi coverage to 0.0625 ML due to reduced through-space and through-surface Bi–Bi repulsions. Hydrogen chemisorption [25,26] and surface characterisation studies for vapour-deposited Bi on Pt(111) surfaces [27] report Bi adsorption on threefold hollow sites and a desorption barrier of 340 kJ/mol under zero coverage limit. Hence, our results for Bi adatom configuration/Pt(111) are in agreement with the previous experimental literature.

Repulsive lateral interactions between Bi atoms for sub-ML coverage were reported experimentally [27,28], and as a result, Bi atoms disperse more uniformly on Pt(111) as compared with other transition metals [29]. Bond dissociation energies of Pt–Pt, Pt–Bi and Bi–Bi metal atom dimers were determined to be 329, 314 and 251 kJ/mol, respectively. The corresponding bond lengths for these dimers are 2.350, 2.434 and 2.656 Å. These dissociation energy values also indicate strong binding between Pt and Bi atoms as compared with Bi–Bi formation. Thus, Bi atoms are more likely to form clusters with Pt atoms or remain dispersed rather than form inactive Bi islands on Pt surface.

Previous literature investigations suggest that both adatom and bulk atom deposition are favoured thermodynamically, but adatom formation is kinetically more favourable when low Bi^{3+} concentrations are used for deposition [8]. Hence, dopant configurations are also dependent on catalyst preparation methods. Furthermore, experimental studies conclude that Bi adsorption on Pt substrates is irreversible when Pt electrodes are modified by dipping into solutions with suitable cations [8,14]. Thus, adatom configurations can be considered irreversible with no mobility on Pt(111) surface.

We have evaluated the relative stability and net charge transfer for both Bi dopant configurations on an orthogonal (4×4) unit cell of Pt(111) surface (which corresponds to

$2\sqrt{3} \times 4$ supercell with 16 atoms/layer). In the adatom configuration, Bi is adsorbed on the hcp site, and in the surface dopant configuration we collated the energies of $\text{Pt}_{15}\text{Bi}/\text{Pt}(111)$ surface alloy and a bulk Pt metal atom. Bi adsorption as an adatom is found to be energetically more stable than the surface dopant composition by 52 kJ/mol. Although Bi adatoms are favoured energetically, dopant configurations can vary depending on preparation method such that one or both configuration phases may be present on the metal substrate. Charge transfer analysis for Bi surface dopant and adatom configurations on Pt(111) surfaces indicates fractional electron transfer from Bi atom to Pt surface. Bi surface dopant and adatom contribute 0.84 and 0.64 e to Pt(111) surface, respectively. Hence, our results confirm that Pt surface remains in reduced form after Bi doping.

3.2 Adsorbate energetics and CO oxidation kinetics on PtBi surface alloy

Figure 1(a) shows the atop, bridge, fcc and hcp binding sites examined on (2×2) unit cell of Pt_3Bi (111) surface alloy. BEs and structural details for optimised CO and O geometries on this surface alloy and pure Pt(111) surface are reported in Table 1. In general, CO and O binding is determined to be weakened by doping Pt(111) surface with Bi atoms.

CO adsorbs most strongly on threefold hollow F1 and H1 sites on Pt(111) surface. These sites are retained as the lowest energy configurations for CO adsorption on PtBi(111) surface alloy although the BEs are reduced significantly. CO adsorption on bridge and hollow sites composed of Pt and Bi atoms results in CO shifting to Pt only atop and bridge sites, respectively. CO molecule is strongly repelled by Bi dopant atom such that atop adsorption on Bi (A2 site) results in CO desorption from surface. Thus, Bi as a surface dopant creates a CO

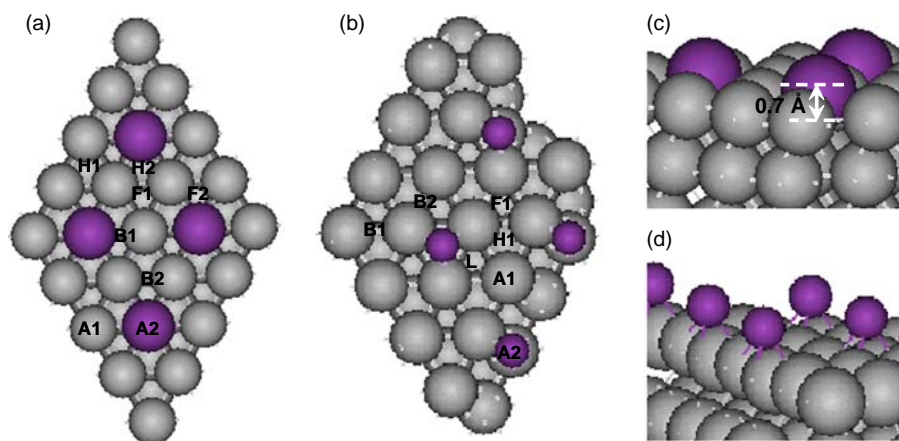


Figure 1. Top and side views for Bi-doped Pt(111) surfaces: (a) and (c) Bi as a surface dopant and (b) and (d) Bi as an adatom. Atop (A1, A2), bridge (B1, B2), fcc (F1, F2), hcp (H1, H2) and hollow (L) adsorption sites are indicated in the figures.

Table 1. BE and bond distances (Pt–C, Pt–O) for CO and O adsorbed on Pt(111) and Bi-promoted Pt(111) surfaces.

Adsorption site	Site details	CO binding energy (kJ/mol) ($d_{\text{Pt-C}}$, Å)		
		Pt(111)	Bi surface dopant/Pt	Bi adatom/Pt
A1	Atop Pt	–132 (1.846)	–81 (1.857)	–67 (1.841)
A2	Atop Bi		–2 (Bi–C: 4.230)	Desorbs
B1	Bridge Pt–Bi		Atop Pt	Bridge Pt–Pt: –61 (2.002, 2.002)
B2	Bridge Pt–Pt	–137 (2.025, 2.025)	–89 (2.042, 2.042)	–49 (1.959, 2.051)
F1	fcc Pt–Pt–Pt	–133 (2.121, 2.121, 2.122)	–92 (2.151, 2.151, 2.152)	–78 (2.097, 2.097, 2.098)
H1	hcp Pt–Pt–Pt		–93 (2.144, 2.144, 2.144)	–70 (2.062, 2.078, 2.078)
F2/L	fcc/hollow Pt–Pt–Bi		Bridge Pt–Pt	Atop Pt
H2	hcp Pt–Pt–Bi		Bridge Pt–Pt	
			O binding energy (kJ/mol) ($d_{\text{Pt-O}}$, Å)	
Adsorption site	Site details	Bi surface dopant/Pt		
		Pt(111)		
A1	Atop Pt	26 (1.822)	71 (1.864)	–10 (1.904)
A2	Atop Bi		51 (1.971)	69 (1.960)
B1	Bridge Pt–Bi		BiO*	fcc Pt–Pt–Pt
B2	Bridge Pt–Pt	fcc Pt–Pt–Pt	BiO*	BiO*
F1	fcc Pt–Pt–Pt	–106 (2.050, 2.050, 2.050)	–54 (2.101, 2.101, 2.100)	9 (2.060, 2.060, 2.061)
H1	hcp Pt–Pt–Pt	–49 (2.063, 2.063, 2.064)	–20 (2.137, 2.138, 2.138)	BiO*
F2/L	fcc/hollow Pt–Pt–Bi		BiO*	BiO*
H2	hcp Pt–Pt–Bi		BiO*	

prohibited zone in its local vicinity (Appendix 1) and effectively blocks CO from binding on nearby active Pt sites (geometric effect).

Atomic oxygen preferentially adsorbs on fcc sites on Pt(111) surface. Similar to CO adsorption, O binds most strongly on pure Pt fcc site (F1) although Pt–O bonds are weakened to a great extent in the presence of Bi surface dopant. When atomic oxygen is adsorbed on bridge and threefold hollow sites with both Pt and Bi atoms, BiO is formed. Due to the lattice mismatch between Pt and Bi, doping the Pt substrate induces strain in the structure. Hence, Bi surface atom can be pulled out of the surface in the presence of O* to form thermodynamically favourable oxide-like structure.

This decrease in CO and O BEs on PtBi surface alloy can be attributed to electronic structure changes in the metal substrate caused by the dopant atom. The calculated d-band centres for Pt(111) and Pt₃Bi(111) surface alloy are -2.14 and -2.27 eV below the Fermi level, respectively (Appendix 2). Due to the lower d-band centre for the surface alloy, overlap between metal d-band and adsorbate states decreases, resulting in weaker binding. Other theoretical studies have also invoked d-band centre calculations to explain binding energy trends on metal alloys [30,31]. This adsorbate–Pt bond weakening on PtBi surface alloys is found to be a local effect which depends on the Bi loading levels on Pt surface. CO binding energy comparisons on Pt₃Bi (2×2 unit cell) and Pt₁₅Bi (orthogonal 4×4 unit cell) surface alloys show that Bi dopant is less prohibitive against CO poisoning for lower Bi/Pt ratios in the top slab layer (Appendix 4). Similar conclusions are drawn by comparing CO binding on bulk PtBi and PtBi₂ alloys [11] and Pt₃Sn surfaces which are resistant to CO poisoning [32].

We have next examined the effect of Bi surface dopant on the elementary reactions for LH-based CO oxidation mechanism. We have considered both O₂ dissociation and surface reaction between CO and O on Pt₁₅Bi (orthogonal 4×4 unit cell) surface alloy. The reactant, TS and product structures for these elementary reactions are shown in Figure 2. Pt–C and Pt–O bond distances in the TS structure are reported in Table 2 along with the associated activation barrier for the elementary reaction.

Both O₂ dissociation and CO oxidation surface reactions are highly exothermic on PtBi surface alloy. Although O₂ dissociation involves an early TS structure (i.e. TS structure is close to initial state (IS) structure), CO oxidation has a late TS structure. O₂ dissociation on Pt(111) surface proceeds via a weakly bound molecular precursor state (-36 kJ/mol) such that O–O bond lies over an fcc site (Appendix 3(a)). In contrast, the most stable site for O₂ molecular precursor on PtBi surface alloy (Figure 2(a)) involves oxygen atoms on atop Pt sites (nearby Bi dopant atom) such that O–O bond lies over a bridge site with a BE of -29 kJ/mol. TS structure involves oxygen atoms on atop positions which relax to mixed Pt–Pt–Bi hcp sites after complete dissociation (Figure 2(b) and (c)). CO oxidation was then examined for an atop adsorbed CO molecule in the presence of these two dissociated oxygen atoms (Figure 2(d)). TS for CO oxidation surface reaction includes shifting of one of the oxygen atoms to a bridge position so as to form C–O bond, whereas the second oxygen atom continues to sit at the Pt–Pt–Bi hcp site (Figure 2(e)). CO₂ thus formed readily desorbs from the surface alloy leaving behind a dissociated oxygen atom.

O₂ dissociation on Pt₁₅Bi surface alloy corresponds to a barrier of 24 kJ/mol with respect to the molecular precursor. Although this barrier is slightly lower than O₂

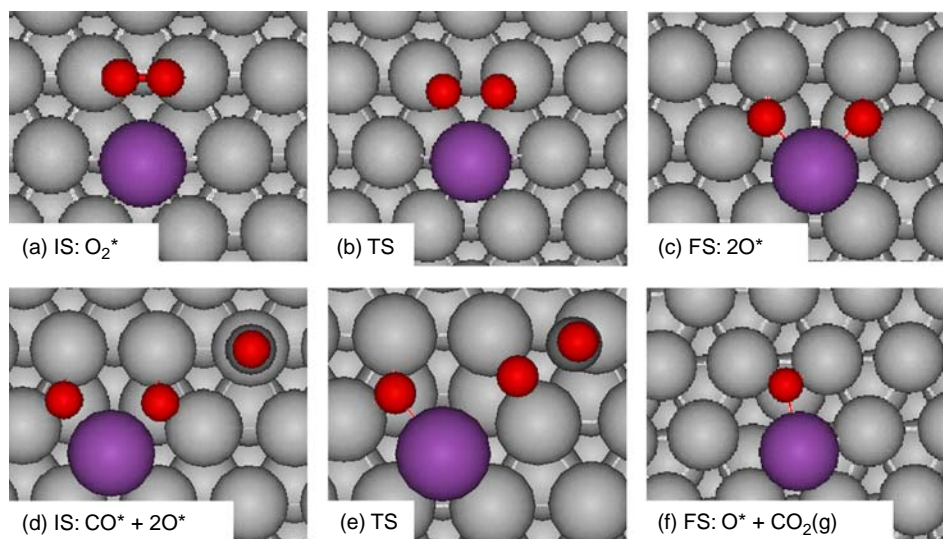


Figure 2. IS, TS and final state (FS) structures for (a–c) O₂ dissociation and (d–f) CO oxidation on Bi doped Pt(111) surface alloy.

Table 2. Kinetic barriers (E_a), enthalpy (H) and TS bond distances for elementary reactions on Pt(111) and Bi-doped Pt(111) surfaces. T and B refer to the distance between Pt atoms and top and bridge bonded adsorbates, respectively.

	E_a (kJ/mol)	H (kJ/mol)	$d_{\text{Pt}-\text{C}}$ (Å)	$d_{\text{Pt}-\text{O}}$ (Å)	$d_{\text{Bi}-\text{O}}$ (Å)	$d_{\text{reacting atoms}}$ (Å)
Pt(111)						
$\text{O}_2(\text{g}) \rightarrow 2\text{O}^*$	2	-93		T: 1.850 B: 2.007, 2.007		2.060
$\text{CO}^* + \text{O}^* \rightarrow \text{CO}_2(\text{g})$	80	-76	1.911	2.050, 2.050		2.040
<i>Bi surface dopant/Pt(111)</i>						
$\text{O}_2(\text{g}) \rightarrow 2\text{O}^*$	-5	-149		1.929 (T), 1.929 (T) B: 2.075, 2.078	2.58, 2.58	1.830
$\text{CO}^* + \text{O}^* \rightarrow \text{CO}_2(\text{g})$	64	-86	1.932	B (BiO*): 2.063, 2.089	2.278	1.910
<i>Bi adatom/Pt(111)</i>						
$\text{BiO}_2^* \rightarrow \text{BiO}^* + \text{O}^*$	59	-150	Pt-Bi: 2.682, 2.763	2.087, 2.133	2.130	1.730
$\text{Bi}^* + \text{O}_2(\text{g}) \rightarrow \text{BiO}^* + \text{O}^*$	-7	-160	Pt-Bi: 2.685, 2.690, 2.703, 1.945	T: 1.905 B: 2.046, 2.047	3.470	1.820
$\text{BiO}^* + \text{CO}^* \rightarrow \text{Bi}^* + \text{CO}_2(\text{g})$	55	-106	(Pt-Bi: 2.665, 2.719, 3.030)	2.066	2.239	1.870

dissociation barrier on pure Pt(111) surface (38 kJ/mol), dissociated oxygen atoms on Bi-doped surface lead to considerably more exothermic reaction. CO oxidation barrier has also reduced on PtBi surface alloy and this can be attributed to weaker Pt-CO and Pt-O binding values. Figure 3 compares the overall thermodynamics for CO oxidation mechanism on PtBi surface alloy with pure Pt surface. As is evident from the figure, dissociated oxygen atoms are adsorbed more strongly on PtBi surface alloy due to BiO* formation. The TS energy for the subsequent CO oxidation step is much more stabilised on the surface alloy than on the Pt surface. Thus, we can conclude that CO oxidation on PtBi surface alloy will proceed more readily than that on pure Pt surface.

3.3 Adsorbate energetics and CO oxidation kinetics on Bi adatom/Pt(111)

Bi adatom preferentially adsorbs on hcp sites on Pt(111) surface, and the nearby binding sites available for adsorbate binding on a (2×2) unit cell are indicated in Figure 1(b). BEs for CO and O geometries reported in Table 1 for Bi adatom configuration correspond to a further weakening of metal-adsorbate bonds as compared with Pt₃Bi (111) surface alloy on account of an increase in interatomic repulsions.

The lowest energy configurations for CO binding on Bi adatom/Pt(111) surface are threefold pure Pt hollow sites (F1 and H1). This result is consistent with the conclusions from Bi surface dopant configuration such that Bi reduces CO adsorption on nearby Pt sites. CO adsorption on hollow site L composed of Pt and Bi atoms results in CO shifting to an atop Pt position. Bi adatom, therefore, continues to repel CO adsorbates and weakens CO binding, but has a more confined CO prohibited zone. In contrast, atomic oxygen readily forms BiO with the Bi adatom/Pt(111) surface. The Bi-O bond length within this suboxide equals 2.137 Å such that Bi sits on a bridge site (Pt-Bi: 2.699 Å, 2.700 Å) while O binds to an atop Pt site (2.037 Å).

We have next investigated the O₂ dissociation mechanisms on Bi adatom/Pt(111) surface on a $p(4 \times 4)$ unit cell. Since Bi favours Bi-O bond formation, we have considered two competing routes to obtain dissociated oxygen atoms. The first route involves BiO₂ formation followed by O-O scission, whereas the second route involves a concerted reaction between Bi adatom and O₂ molecular precursor. The reactant, TS and product structures for these elementary reactions are shown in Figure 4(a)-(e) and the associated barriers are included in Table 2.

BiO₂ formation on Pt(111) surface is exothermic with a weak binding energy of -12 kJ/mol such that one end of the O₂ molecule forms Bi-O bond with Bi adatom

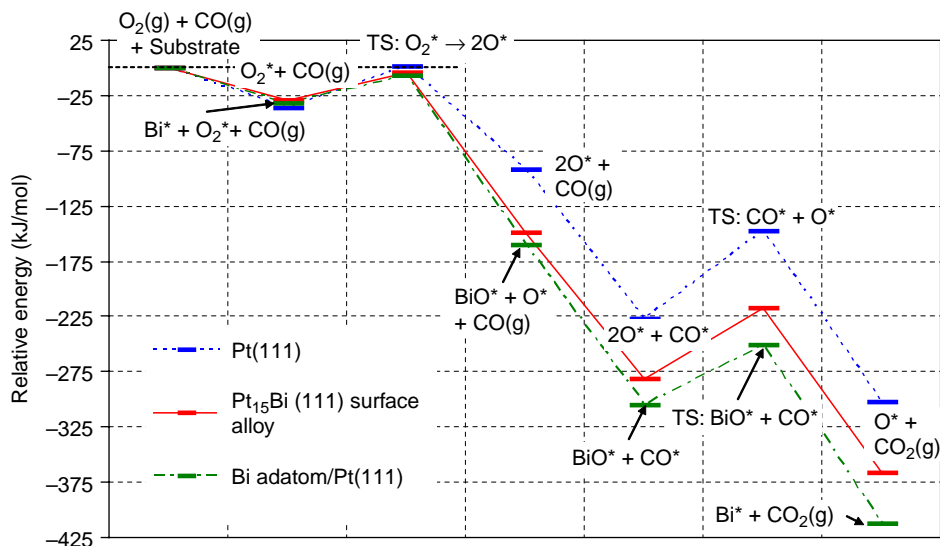


Figure 3. Reaction energetics for LH CO oxidation mechanism on Pt(111), Bi-doped Pt(111) surface alloy and Bi adatom/Pt(111) surface.

whereas the second oxygen terminal adsorbs on an adjoining atop Pt site (Figure 4(a)). Although Pt–O bond distance equals 2.018 Å, Bi–O and O–O bond distances correspond to 2.371 and 1.361 Å, respectively (Pt–Bi:

2.703 Å, 2.706 Å, 2.864 Å). TS for O–O scission within BiO₂ molecule involves an increase in O–O bond distance, whereas Bi adheres to bridge site and oxygen atom is bridged on Pt atoms (Figure 4(b)). In the final

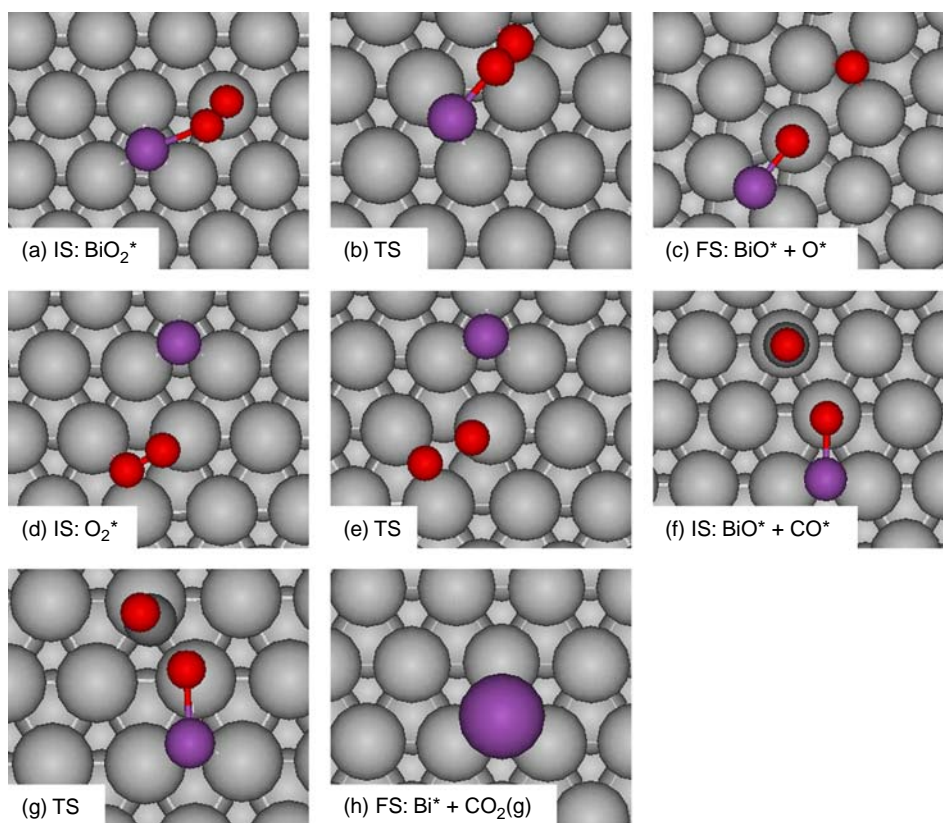


Figure 4. IS, TS and FS structures for BiO₂* → BiO* + O* (a)–(c), Bi* + O₂* → BiO* + O* (d), (e) and (c) and BiO* + CO* → Bi* + CO₂(g) (g) and (h) on Bi adatom/Pt(111) surface.

dissociated structure shown in Figure 4(c), both BiO and O adsorb across fcc sites.

For the $\text{Bi}^* + \text{O}_2 \rightarrow \text{BiO}^* + \text{O}^*$ reaction, the precursor O_2 adsorbs weakly with a binding energy of -31 kJ/mol and the O—O bond over a fcc site (Figure 4(d)). The TS structure (Figure 4(e)) is very similar to the TS structure on Pt(111) surface such that on relaxation, one of the oxygen atoms forms a Bi—O bond, whereas the second one remains in an fcc position (Figure 4(c)).

We next considered the CO oxidation reaction wherein CO molecule can extract the oxygen atom from BiO to form CO_2 and reduced Bi adatom. TS for CO oxidation surface reaction includes CO tilting towards the oxygen end of BiO molecule, whereas Pt—C bond is elongated (Figure 4(g)). CO_2 thus formed can readily desorb from the surface whereas Bi returns to its reduced form.

On the basis of the reaction kinetics, BiO_2^* dissociation involves a high barrier of 59 kJ/mol, whereas $\text{Bi}^* + \text{O}_2^*$ has a low barrier of 24 kJ/mol, with respect to the chemisorbed O_2 precursor. Hence, the CO oxidation mechanism on Bi adatom/Pt(111) proceeds via $\text{Bi}^* + \text{O}_2 \rightarrow \text{BiO}^* + \text{O}^*$ followed by $\text{BiO}^* + \text{CO}^* \rightarrow \text{Bi}^* + \text{CO}_2$ (g). The overall reaction barrier for CO oxidation on this dopant configuration results in a lower energy pathway than PtBi surface alloy barrier as shown in Figure 3. Hence, CO oxidation is established to be more favourable on Bi-modified Pt surfaces irrespective of the Bi dopant configuration.

On the basis of this *ab initio* study, we have determined that Bi plays a dual role in CO oxidation mechanism on Pt(111) surface. On the one hand, it acts as an inert site blocker for CO molecules due to the electronic and geometric effect of Bi doping on Pt substrate. On the other hand, Bi actively participates in O_2 dissociation and CO oxidation elementary reactions via BiO suboxide formation. Bi dopants, therefore, effectively reduce the active Pt ensemble size available for CO adsorption such that lower CO coverage results in doped Pt(111) surfaces. This coverage reduction has been confirmed experimentally via low intensity and high temperature desorption peaks in CO temperature programmed desorption studies and low C—O stretching frequencies in high-resolution electron energy loss spectroscopic experiments on Bi/Pt(111) [29]. O_2 dissociation barriers on both PtBi surface alloy and in the presence of Bi adatom are slightly lower than kinetics on Pt surface. However, Bi-doped Pt surfaces enhance O_2 dissociation indirectly by making available larger active site areas for O_2 adsorption and dissociation as compared with pure Pt. This site area on Bi-doped Pt(111) includes the CO-prohibited zone and the sites from which CO molecules desorb at lower temperatures due to weaker BEs. XPS and HREELS studies support this hypothesis by reporting significant O_2 dissociation enhancement and minimal reduction in O_2 adsorption energies with an increase in Bi coverage on Pt(111) surface [29].

Furthermore, work function increase observed experimentally with oxygen adsorption on these doped surfaces indicates that oxygen atoms are in fact adsorbed on the surface instead of subsurface sites and can, therefore, participate in surface CO oxidation reaction. Hence, catalytic properties for Bi-modified Pt surfaces are controlled by simultaneous weakening of CO adsorption and preferential oxygen adsorption near dopant atoms.

4. Conclusions

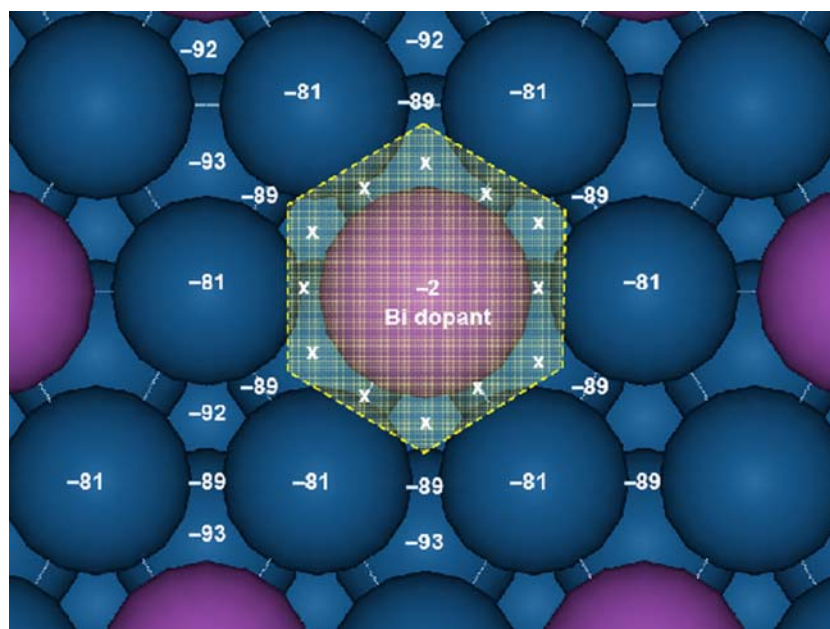
First-principles-based simulations were used to investigate the electronic and geometric effects of Bi-promoted Pt(111) surface on CO oxidation mechanism. Bi adatom preferentially adsorbs on threefold hollow sites on Pt(111) and is thermodynamically more favourable than Bi as a surface dopant. However, for both dopant configurations, Bi atom repels CO molecule and alters the electronic structure of adjacent Pt sites to create a local CO-free zone whose area varies with doping levels. O_2 molecule can adsorb within this CO-prohibited area in the vicinity of Bi dopant and undergo O—O dissociation. Atomic oxygen atoms thus obtained form BiO suboxide with nearby Bi adatoms. A concerted reaction between BiO and CO results in reduced Bi and CO_2 with low barrier requirements as compared with Pt(111) surface. Adsorbate energies (CO, O) are significantly reduced on these promoted surfaces due to lower d-band centre energy for PtBi surface. Thus, Bi promoter leads to improved CO oxidation performance on account of its favourable impact on CO oxidation energetics and kinetics while suppressing CO poisoning effect.

References

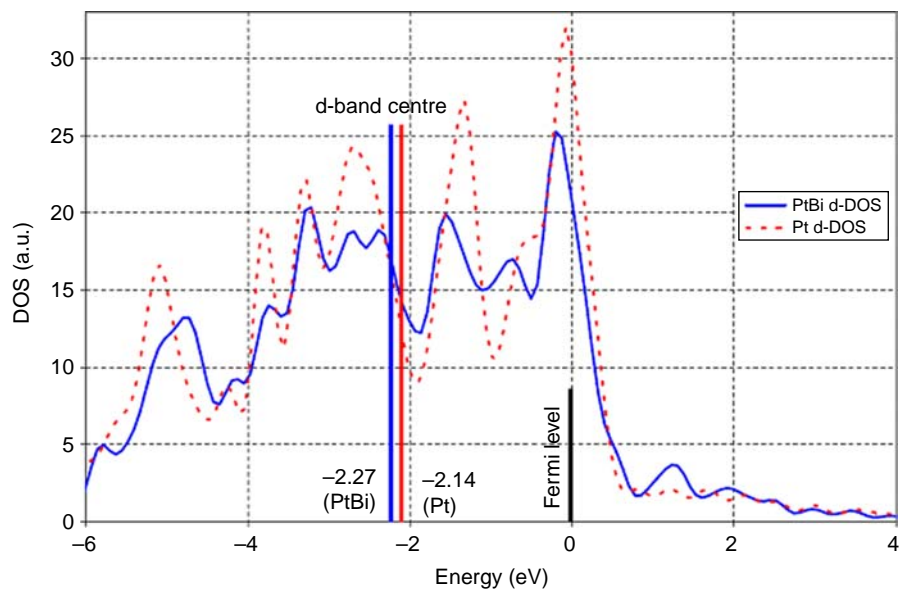
- [1] B. Shan, Y. Zhao, J. Hyun, N. Kapur, J.B. Nicholas, and K. Cho, *Coverage-dependent CO adsorption energy from first-principles calculations*, J. Phys. Chem. C 113 (2009), pp. 6088–6092.
- [2] M.Ø. Pedersen, M.-L. Bocquet, P. Sautet, E. Lægsgaard, I. Stensgaard, and F. Besenbacher, *CO on Pt(111): Binding site assignment from the interplay between measured and calculated STM images*, Chem. Phys. Lett. 299 (1999), pp. 403–409.
- [3] Y.Y. Yeo, L. Vattuone, and D.A. King, *Calorimetric heats for CO and oxygen adsorption and for the catalytic CO oxidation reaction on Pt(111)*, J. Chem. Phys. 106 (1997), pp. 392–401.
- [4] H. Froitzheim, H. Hopster, H. Ibach, and S. Lehwald, *Adsorption sites of CO on Pt(111)*, Appl. Phys. A 13 (1977), pp. 147–151.
- [5] B. Shan, N. Kapur, J. Hyun, L. Wang, J.B. Nicholas, and K. Cho, *CO-coverage-dependent oxygen dissociation on Pt(111) surface*, J. Phys. Chem. C 113 (2009), pp. 710–715.
- [6] D.J. Burnett, A.T. Capitano, A.M. Gabelnick, A.L. Marsh, D.A. Fischer, and J.L. Gland, *In-situ soft X-ray studies of CO oxidation on the Pt(111) surface*, Surf. Sci. 564 (2004), pp. 29–37.
- [7] P.J. Berlowitz, C.H.F. Peden, and D.W. Goodman, *Kinetics of carbon monoxide oxidation on single-crystal palladium, platinum, and iridium*, J. Phys. Chem. 92 (1988), pp. 5213–5221.
- [8] T. Mallat, Z. Bodnar, P. Hug, and A. Bäiker, *Selective oxidation of cinnamyl alcohol to cinnamaldehyde with air over Bi—Pt/alumina catalysts*, J. Catal. 153 (1995), pp. 131–143.

- [9] C. Keresszegi, T. Mallat, J. Grunwaldt, and A. Baiker, *A simple discrimination of the promoter effect in alcohol oxidation and dehydrogenation over platinum and palladium*, *J. Catal.* 225 (2004), pp. 138–146.
- [10] H. Kimura, K. Tsuto, T. Wakisaka, Y. Kazumi, and Y. Inaya, *Selective oxidation of glycerol on a platinum–bismuth catalyst*, *Appl. Catal. A* 96 (1993), pp. 217–228.
- [11] M. Oana, R. Hoffmann, H.D. Abruña, and F.J. DiSalvo, *Adsorption of CO on PtBi2 and PtBi surfaces*, *Surf. Sci.* 574 (2005), pp. 1–16.
- [12] D.R. Blasini, D. Rochefort, E. Fachini, L.R. Alden, F.J. DiSalvo, C.R. Cabrera, and H.D. Abruña, *Surface composition of ordered intermetallic compounds PtBi and PtPb*, *Surf. Sci.* 600 (2006), pp. 2670–2680.
- [13] E. Casado-Rivera, Z. Gál, A.C.D. Angelo, C. Lind, F.J. DiSalvo, and H.D. Abruña, *Electrocatalytic oxidation of formic acid at an ordered intermetallic PtBi surface*, *ChemPhysChem* 4 (2003), pp. 193–199.
- [14] T.J. Schmidt, B.N. Grgur, R.J. Behm, N.M. Markovic, and P.N. Ross, Jr, *Bi adsorption on Pt(111) in perchloric acid solution: A rotating ring-disk electrode and XPS study*, *Phys. Chem. Chem. Phys.* 2 (2000), pp. 4379–4386.
- [15] M. Horiuchi and T. Yokomizo, *Catalyst for purification of diesel engine exhaust gas*, US patent 5911961, issued June 15 1999.
- [16] J. Jia, K.L. Furdala, and T.J. Truex, *Platinum–bismuth catalysts for treating engine exhaust*, US patent 7605109 B1, issued Oct 20 2009.
- [17] T.N. Taylor, C.T. Campbell, J.W. Rogers, Jr, W.P. Ellis, and J.M. White, *The interaction of oxygen with Bi(0001): Kinetic, electronic, and structural features*, *Surf. Sci.* 134 (1983), pp. 529–546.
- [18] M. Kinne, A. Heidenreich, and K. Rademann, *Reactions of selected bismuth oxide cluster cations with propene*, *Ang. Chem. Int. Ed.* 37 (1998), pp. 2509–2511.
- [19] M. Bienati, V. Bonacic-Koutecky, and P. Fantucci, *Theoretical study of the reactivity of bismuth oxide cluster cations with ethene in the presence of molecular oxygen*, *J. Phys. Chem. A* 104 (2000), pp. 6983–6992.
- [20] G. Kresse and J. Furthmüller, *Efficient iterative schemes for ab initio total-energy calculations using a plane-wave basis set*, *Phys. Rev. B* 54 (1996), p. 11169.
- [21] H.J. Monkhorst and J.D. Pack, *Special points for Brillouin–zone integrations*, *Phys. Rev. B* 13 (1976), p. 5188.
- [22] P.E. Blöchl, *Projector augmented-wave method*, *Phys. Rev. B* 50 (1994), p. 17953.
- [23] G. Henkelman and H. Jonsson, *A dimer method for finding saddle points on high dimensional potential surfaces using only first derivatives*, *J. Chem. Phys.* 111 (1999), pp. 7010–7022.
- [24] G. Henkelman, A. Arnaldsson, and H. Jonsson, *A fast and robust algorithm for Bader decomposition of charge density*, *Comput. Mater. Sci.* 36 (2006), pp. 254–360.
- [25] J. Clavilier, J.M. Feliu, and A. Aldaz, *An irreversible structure sensitive adsorption Step in bismuth underpotential deposition at platinum electrodes*, *J. Electroanal. Chem.* 243 (1988), pp. 419–433.
- [26] N. Furuya and S. Motoo, *Arrangement of Ad-atoms of various kinds on substrates: Part I. Platinum substrate*, *J. Electroanal. Chem.* 98 (1979), pp. 189–194.
- [27] M.T. Paffett, C.T. Campbell, and T.N. Taylor, *Adsorption and growth modes of Bi on Pt(111)*, *J. Chem. Phys.* 85 (1986), p. 6176.
- [28] M.T. Paffett, C.T. Campbell, and T.N. Taylor, *The influence of adsorbed Bi on the chemisorption properties of Pt(111): H₂, CO, and O₂*, *J. Vac. Sci. Technol. A* 3 (1985), pp. 812–816.
- [29] M.T. Paffett, C.T. Campbell, R.G. Windham, and B.E. Koel, *A multitechnique surface analysis study of the adsorption of H₂, CO and O₂ on surfaces*, *Surf. Sci.* 207 (1989), pp. 274–296.
- [30] R.M. Watwe, R.D. Cortright, M. Mavrikakis, J.K. Norskov, and J.A. Dumesic, *Density functional theory studies of the adsorption of ethylene and oxygen on Pt(111) and Pt3Sn(111)*, *J. Chem. Phys.* 114 (2001), p. 4663.
- [31] M. Mavrikakis, B. Hammer, and J.K. Norskov, *Effect of strain on the reactivity of metal surfaces*, *Phys. Rev. Lett.* 81 (1998), p. 2819.
- [32] M.A. Gülmen, A. Sümer, and A.E. Aksoylu, *Adsorption properties of CO on low-index Pt3Sn surfaces*, *Surf. Sci.* 600 (2006), pp. 4909–4921.

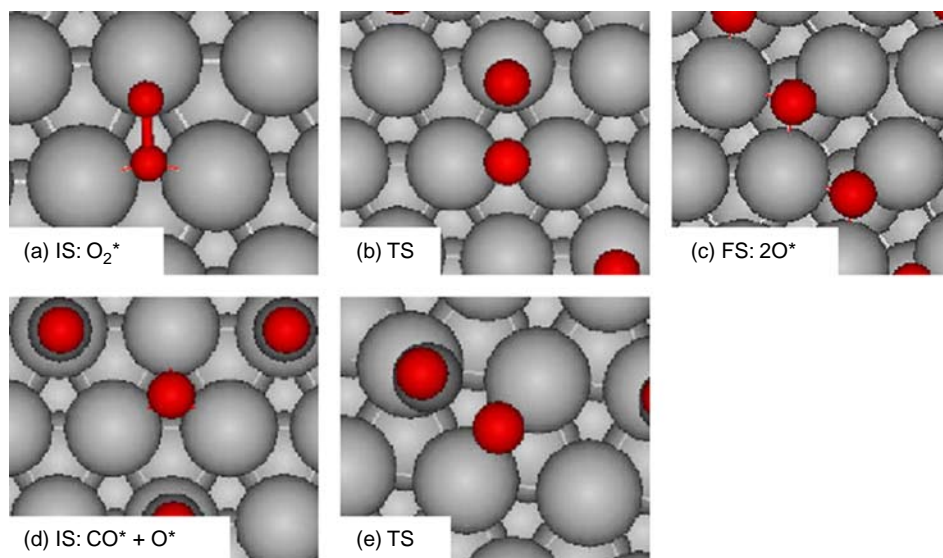
Appendices



Appendix 1. Highlighted area represents the CO-prohibited zone for Pt₃Bi(111) surface alloy. CO binding energies (kJ/mol) on the different Pt and Bi-based adsorption sites are indicated on the surface alloy structure.



Appendix 2. Density of states (DOS) plot for Pt(111) and Pt₃Bi(111) surface alloy.



Appendix 3. IS, TS and FS structures for (a)–(c) O₂ dissociation and (d) and (e) CO oxidation on Pt(111) (2 × 2 unit cell) surface.

Appendix 4. CO and O binding energies on Pt₃Bi(111) and Pt₁₅Bi(111) surface alloys.

Adsorption site	Site details	CO binding energy (kJ/mol)		
		Pt(111)	Pt ₃ Bi	Pt ₁₅ Bi
A1	Atop Pt	-132	-81	-118
A2	Atop Bi		-2	Desorbs
B1	Bridge Pt-Bi		Atop Pt	-113
B2	Bridge Pt-Pt	-137	-89	-133
F1	fcc Pt-Pt-Pt	-133	-92	-140
H1	hcp Pt-Pt-Pt	-134	-93	-133
F2	fcc Pt-Pt-Bi		Bridge Pt-Pt	-119
H2	hcp Pt-Pt-Bi		Bridge Pt-Pt	-115
O binding energy (kJ/mol)				
Adsorption site	Site details	Pt(111)	Pt ₃ Bi	Pt ₁₅ Bi
A1	Atop Pt	26	71	-17
A2	Atop Bi		51	Desorbs
B1	Bridge Pt-Bi		BiO*	-12
B2	Bridge Pt-Pt	fcc Pt-Pt-Pt	BiO*	fcc Pt-Pt-Pt
F1	fcc Pt-Pt-Pt	-106	-54	-90
H1	hcp Pt-Pt-Pt	-49	-20	-51
F2	fcc Pt-Pt-Bi		BiO*	BiO*
H2	hcp Pt-Pt-Bi		BiO*	BiO*